CHAPTER

Principle of photovoltaics 1

Nowshad Amin
Institute of Sustainable Energy, Universiti Tenaga Nasional (@UNITEN; The Energy University), Kajang, Malaysia

1.1 Introduction

In this chapter, the characteristics and amount of the sun's energy as the main input source of solar photovoltaic (PV) energy will be discussed to show how enormous an energy bank is safely placed millions of kilometers away from us. Then, solar PV fundamentals together and solar cell classification will be introduced for better comprehension of sunlight to electricity conversion. Solar PV cells are electricity generators that differ from more well-known hydroelectric-, diesel- or nuclear reactor-based generators. Energy conversion occurs in a unique way based on the semiconductors' quantum effect, abolishing the need of any heat or mechanical parts as seen in conventional electricity generators. The tremendous growth of solar PV technology over the past few decades has helped the levelized-costs-of-generating-electricity making it very cost competitive among all available electricity-generating sources as shown in Fig. 1.1, which is mainly derived from the rigorous efforts of researchers supported by renewable energy policies around the world as per International Energy Agency (IEA) report. Countries are now including solar PV technology as one of the key contributors in their long term future energy roadmap owing to the confidence gained over the past decade.

1.2 Solar energy

The sun's energy reaches the earth in the form of an electromagnetic wave passing through outer space. The sun is known to be a nuclear fusion reactor and its radiation spectra can be replicated by a perfect black-body heated at 6000K. Considering an average distance of 150 million kilometers between the sun and earth, the incident light on the earth's surface is an assortment of plane electromagnetic waves of various frequencies. The radiation spectra of the sunlight that arrives on the earth's surface is shown in Fig. 1.2, along with the incident light before entering the atmospheric belt of the earth. The solar radiation is attenuated by at least 30% during its passage through the earth's atmospheric belt, where

Comprehensive Guide on Organic and Inorganic Solar Cells. DOI: https://doi.org/10.1016/B978-0-323-85529-7.00015-3

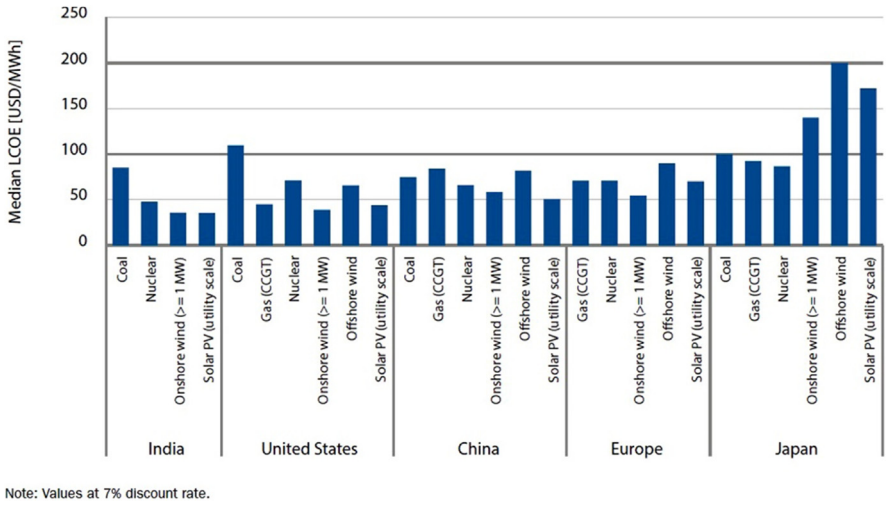

FIGURE 1.1

Median LCOE technology costs by region (data taken from IEA 2020 report).

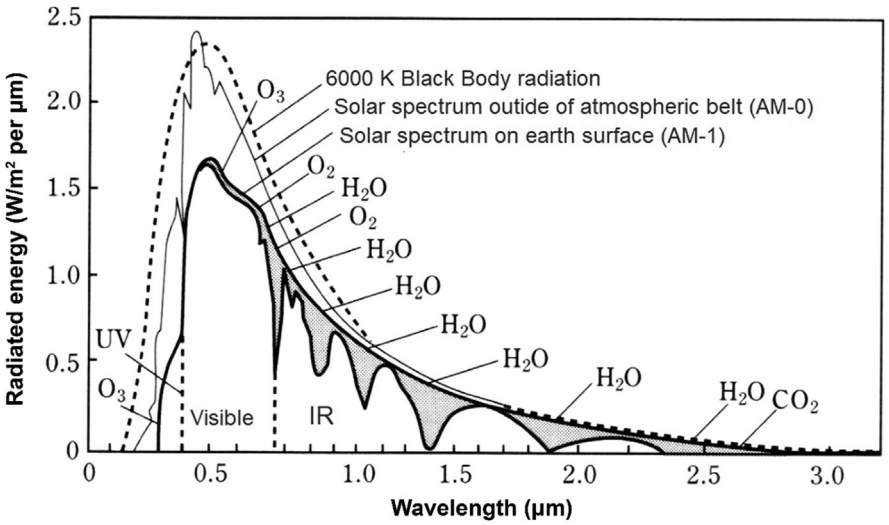

FIGURE 1.2

Solar energy spectra for three different air mass conditions.

most of the energetic ultraviolet or blue waves are reflected by the similarly-sized aerosols in outer space (this is the reason the sky is blue). In addition, the water moisture in the surrounding atmosphere absorbs a substantial amount of incoming solar energy, thereby reducing the amount of sunlight reaching the surface.

To simulate the radiation spectrum of the sun at various places, we use 6000K black-body radiation at the origin (sun), then 5700K black-body radiation for the spectrum on the earth's surface. If we quantify the amount of energy radiated from the sun's surface to electrical power, it equals to 3.8×10^{23} kW, which reaches an energy density of about 1.4 kW/m^2 outside of the earth's atmospheric belt. This energy density is termed as a solar constant. However, the sunlight (energy density) that falls at a location varies depending on the latitude, time, and weather. Again, seasonal variation also changes the sunlight's air-volume in a particular place, which is called Air Mass (AM). It is the shortest and considered unity when the sun is directly overhead and depicted as AM1. AM is 0 in outer space, but for other places on earth, it is derived by the following equation, where θ is the angle of the sun from straight overhead.

$$\text{Air mass} = \frac{1}{\cos\theta} \tag{1.1}$$

Therefore, when the sun is 45 degrees from center, the radiation is AM1.5. One convenient way to estimate AM is to measure the length of the shadow that is cast by any vertical object of height h as shown in the equation below.

$$\text{Air mass} = \sqrt{\left(1 + \left(\frac{s}{h}\right)^2\right)} \tag{1.2}$$

Therefore, the total radiated energy of the sun reaching the earth can be derived from the product of the solar constant with the projected surface area of the earth. One quick example shows that when taking the earth's diameter of 6356 km, the total incident solar energy becomes 177×10^{12} kW. This enormous amount of energy is the total energy from the sun that can be used for various purposes, of which 30% is reflected back to the space. Among the remaining 70% that reaches the earth, around 47% is utilized to keep the earth warm enough for living creatures. Then, the remaining 23% is stored in either seawater or ice with a part of it being used for cloud or rain creation. Among all of these, the energy of energy that is used for wind, wave, or convection energy is only 0.2%, equivalent to 0.37×10^{12} kW. Furthermore, the energy needed for the growth of plants and animals on earth, the photosynthesis of biological systems, is only 0.02% (equivalent to 400×10^8 kW). Nonetheless, these small amounts of solar energy are what is really important for the conservation of the global ecosystem.

To summarize the source of solar energy, it can be concluded that terrestrial sunlight varies dramatically and unpredictably in availability, intensity, and spectral composition. On clear days, the length of the sunlight's path through the atmosphere and the optical AM are important parameters. The indirect or diffuse component of sunlight can be particularly important for less than ideal conditions. Reasonable estimates of global radiation (direct plus diffuse) received annually on horizontal surfaces are available for most regions of the world. There are uncertainties that can be caused by local geographical conditions and approximations involved in the conversion to radiation on inclined surfaces.

1.3 Photovoltaic effect

PV systems comprise the technology to convert sunlight directly into electricity without additional fuel. The term "photovoltaic" is derived from the Greek language. "Photo" means light and "voltaic" means electricity. Charged carriers are produced based on the photo-conduction phenomenon upon incident light on any semiconductor. The light generated carriers will polarize in regions of positively- and negatively-charged particles due to possible diffusion or drift occurring as a result of asymmetric spatial distribution or built-in potential of a p-n junction device and create electromotive forces termed as the PV effect. The PV effect due to spatial non-uniformity of charged carriers has the Dember and photo-electromagnetic effect, but they do not possess a direct relationship with solar PV cells. Therefore, only the PV effect related to the interfacial electric field of the semiconductors will be discussed (Fig. 1.3).

The PV effect is a key to solar energy conversion, where electricity is generated from light energy. Owing to quantum theory, light is regarded as packets of energetic particles called photons, whose energy depends only on light frequency. The energy of visible photons is sufficient to excite electrons and bound into solids up to higher energy levels where they are freer to move. Meanwhile, there are internal electric fields due to the electron affinity and Fermi level between the semiconductor and attached subsequent materials in cases of semiconductor p-n junctions, crystal borders, and semiconductor interfaces or surfaces. Hence, when

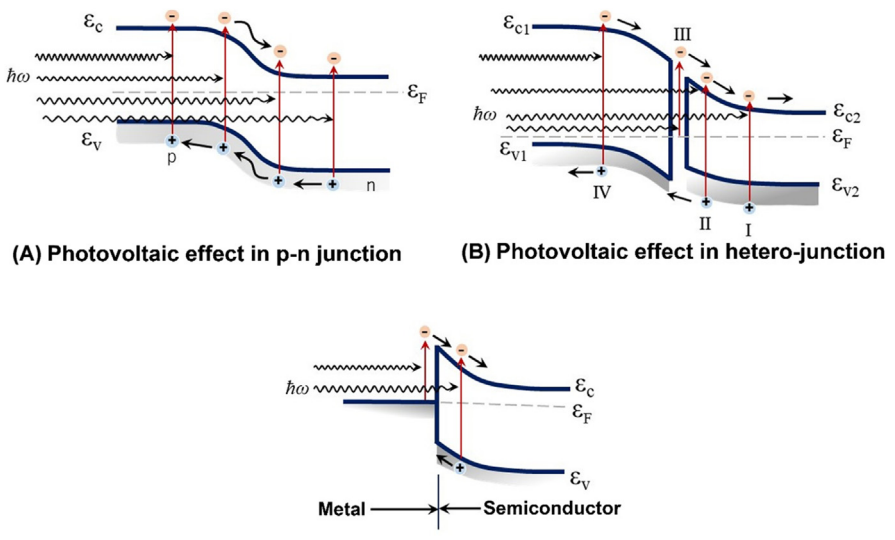

FIGURE 1.3

Photovoltaic effect in various semiconductor junctions and interface.

incoming photons strike such regions, electron-hole pairs are generated that drift in opposite directions to create charge polarization and eventually electromotive force due to light irradiation known as the PV effect. It is only for this PV effect that any semiconductor p-n junctions, heterojunctions, or even Schottky barrier junctions experience interface potential that can create solar cells. On the other hand, many materials possess PV properties but fail to provide ample current due to higher internal resistance for their crystalline structure and are then used as optical sensors. Binary semiconductors, such as ZnO, CdS, ZnSe in sintered form, are used as optical detectors.

1.4 Fundamentals of solar cells

To generate a PV effect, an inbuilt electric potential must exist in semiconductors. The potential that exists between interfaces of materials helps in generating this phenomenon. In general, there is a contact potential between two electronically asymmetric materials. Examples include storage batteries that can generate contact potentials between lead or graphite and electrolytes or thermocouples that use the contact potential differences of two contacted metals. Similarly, contact potential is induced depending on a combination of either semiconductor and metal or semiconductor and semiconductor. The p-n junctions are engineered with good reproducibility with stable combinations of materials that use inherent or inbuilt electric fields in the interfaces (Fig. 1.4).

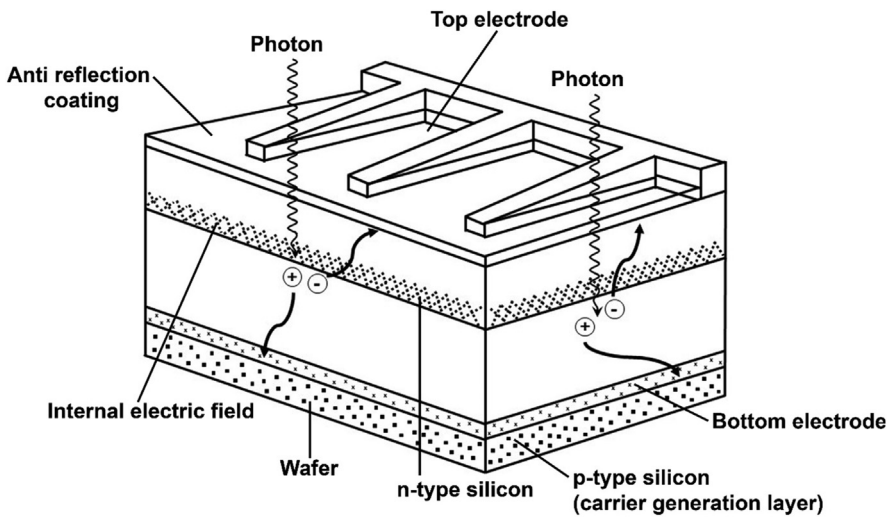

FIGURE 1.4

Structure of a typical crystalline silicon solar cell.

A solar cell is generally a p-n junction with built-in asymmetry that separates the light excited electrons away from the junction region to be extracted out to external circuits. The effectiveness of the solar cell depends on the choice of light absorbing materials as well as supporting materials for the carrier to be efficiently collected through external terminals. To explain basic solar cell fundamentals, only silicon-based solar cells will be inferred in this section. Pure silicon as a group IV semiconductor is undoped, but it must doped with materials that can create either positive (p) type or negative (n) type polarity in silicon. Usually it is done by incorporating group V materials such as P to make n-type silicon and group III materials such as B to make p-type silicon. Silicon doping enhances its electrical conductivity that can easily be controlled or manipulated up to certain limit, which is also called valence electron control typically used in transistor or integrated circuits. If both n-type and p-type silicon are crystallographically joined, then the interface is called the p-n junction. Initial carrier diffusion on both sides of the interface creates a depletion region or space charge region as mobile charges are exhausted due to recombination in the region. This is the reason the internal electric field exists thereby restricting the enhancement of the electric field and pushing any charge carrying particles, for example, electron and hole, on both sides of the p-n junction. A present, all electronic devices such as the diode, transistor, LED, or LASER etc. utilize an internal electric field as the main working principle that originates from the interface potential.

Practically used solar cells are essentially large area p-n junctions that use the interface electric field for the PV effect. A simple silicon solar cell schematic is shown in Fig. 1.3. As seen, the n-type layer is disproportionately thin to allow the incoming light to immediately reach the junction area. As light is illuminated on a solar cell, photons of different wavelengths hit the semiconductor surface, which, in this case, is the n-type silicon region. Only a fraction of the photons are converted into electrical energy, since only photons with energy equal to or greater than the energy bandgap of the semiconductor (Si) are absorbed. Photon absorption leads to the generation of an electron-hole pair, also known as EHP generation. The majority-carrier concentrations (the total number of electrons in an n-type semiconductor or the total number of holes in a p-type semiconductor) are unaffected by photon-assisted carrier generation, as newly generated EHP concentrations are insignificant compared to the majority-carrier concentrations. However, minority-carrier concentrations (the total number of electrons in a p-type semiconductor or the total number of holes in an n-type semiconductor) increase significantly. This change upsets the equilibrium condition between the diffusion force and electrostatic force, resulting in the PV effect. Electrons originating from the p region eventually diffuse into the depletion region, where the potential energy barrier at the junction is lowered, allowing current to flow and establish a voltage at the external terminals. Holes created in the n-doped region travel in the opposite direction to the p-doped side. The generation of charges depending on the incoming photon flux as well as movement of charges in the above manner results in the amount of current density existing along the terminals.

1.5 Energy conversion of solar cells

Energy conversion efficiency (or simply conversion efficiency) of a solar cell, η, is the percentile ratio of output electrical power from the terminals of solar cell to the incident sunlight energy over the same area of the cell. Therefore, the conversion efficiency η can be expressed as the following equation (Fig. 1.5).

$$\eta = \frac{\text{Electrical power output from a solar cell, } P_{out}}{\text{Incident sunlight energy, } P_{in}} \times 100\% \tag{1.3}$$

However, a more difficult procedure is needed to define or derive this conversion efficiency as the solar cell's ultimate performance index. In other words, the conversion efficiency of the same solar cell changes with changes of the incoming light spectra. Moreover, the output energy changes depending on the load connected to the cells even under the same incident light. Therefore, in accordance with IEC TC-82, it is decided to consider the incoming light source under AM 1.5 with incident power of 100 mW/cm^2 for any terrestrial solar cells at maximum power output conditions, which is also termed as nominal efficiency (η_n).

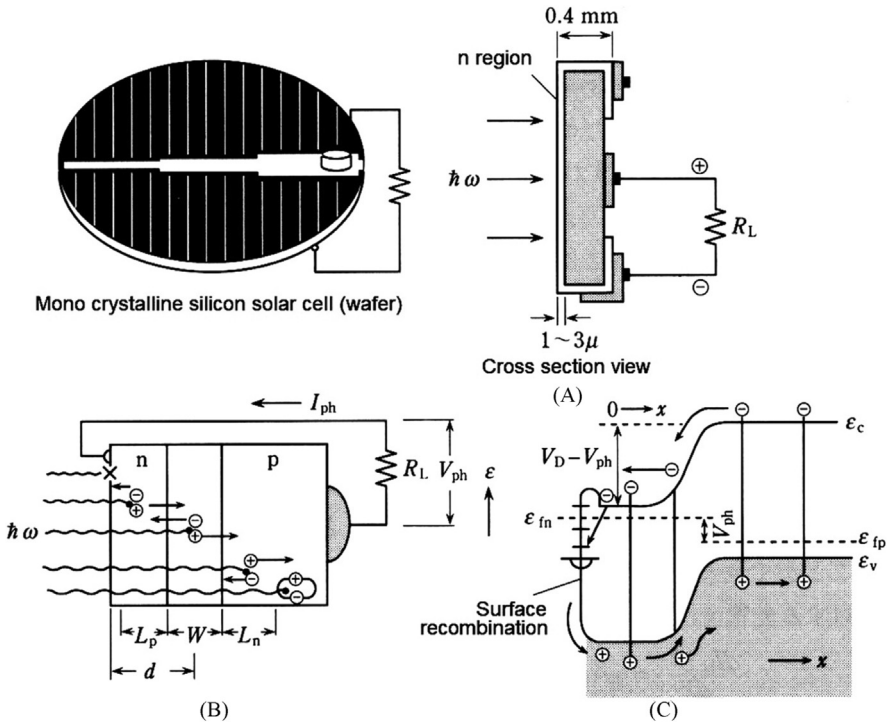

FIGURE 1.5

Working principle of a silicon solar cell (A) cross section of the solar cell, (B) enlarged view of p-n junction and (C) energy band gap diagram showing carrier flow.

The conversion efficiency measured under this condition is usually described in the specifications of solar panels. For publication purposes, we show this value of conversion efficiency. In the derivation of nominal efficiency, it is important to derive the relationships among maximum output power voltage $V_{\max}$ (or V_{mp}), maximum output power current $I_{\max}$ (or I_{mp}), open circuit voltage V_{oc}, and short circuit current density J_{sc} from the measured output characteristics of the solar cell.

When light enters from the surface of a p-n junction type solar cell, the junction exists at a distance, d, from the surface. Considering minority carrier diffusion lengths of both p and n regions as L_n and L_p, the optical absorption coefficient α in respect to the wavelength λ and the opto-electronic quantum efficiency γ, the carrier generation $g(x)$ at a distance from surface x, is proportional to the optical absorption $d\Phi/dx$ as shown in the following equation.

$$g(x) = \gamma\varphi_0\alpha e^{-\alpha x} \tag{1.4}$$

Here, Φ_0 is the optical flux density of the wavelength λ on the surface ($x = 0$). However, in reality, most of the incident light flux generated by the carriers is extinct due to recombination around the surface, $x = 0$, which is known as surface recombination loss. The carriers (both electron and hole) that contribute to the PV effect come from the carriers that are collected due to diffusion from the neutral region border until the length of the minority carrier diffusion (L_n and L_p) on both sides of the depletion region. To determine total photo current, the current in the n-region must be found by integrating the product of $g(x)$ and $\exp[-(d\text{-}x)/L_p]$ from $x = 0$ to d and the current for the p-region and add both components. Consequently, the total current for the monochromatic incident light at the time terminals of both sides are shorted can be found by the following equation.

$$\frac{dI_{sc}(\lambda)}{d\lambda} = \gamma A\alpha\lambda\left\{\frac{L_p}{1-\alpha L_p}\left[e^{-\alpha d} - e^{-d/Lp}\right] + \frac{L_n e^{-\alpha d}}{1-\alpha L_n}\right\} \tag{1.5}$$

In reality, the junction depth is considered much less than the light penetration depth and αL_n, $\alpha L_p \ll 1$, and create the carrier collection effect, so Eq. (1.5) can be simplified as below.

$$\frac{dI_{sc}(\lambda)}{d\lambda} = \gamma A\alpha \cdot \lambda\left(L_n + L_p\right)\mathrm{e}^{-\alpha \mathrm{d}} \tag{1.6}$$

Fig. 1.6 shows an example that compares both the calculated data and experimental data for the spectral response of the silicon solar cell, considering $d = 2\ \mu\text{m}$, $L_n = 0.5\ \mu\text{m}$ and $L_p = 10\ \mu\text{m}$.

In the case of p-n junction type solar cells, the conversion efficiency would be higher when the overlapping increases between the calculated spectral response distribution as shown above and the incident sunlight distribution shown in Fig. 1.2. However, the cutoff wavelength on the longer wavelength side of the spectral response distribution of any material depends on the energy bandgap, whereas the shape of the spectrum depends on the geometrical dimensions of the device, the constants such as L_p, L_n, μ_p, μ_n, and the light absorption coefficient spectra $\alpha(\lambda)$ as shown in Fig. 1.7. Hence, the theoretical limit of the maximum

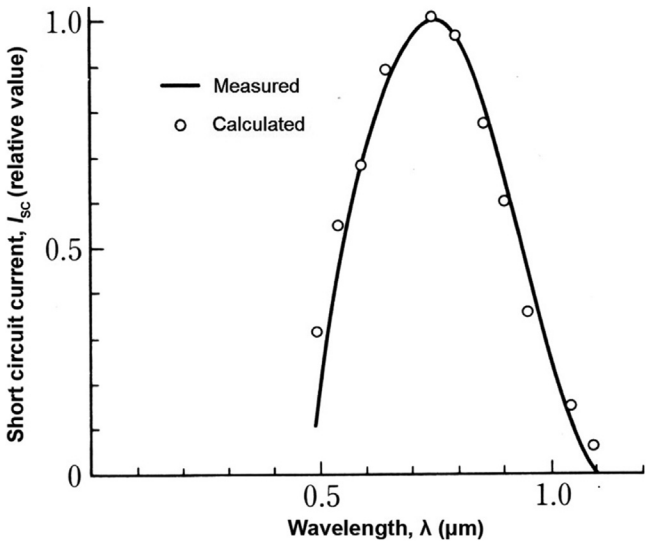

FIGURE 1.6

Spectral response of a silicon solar cell.

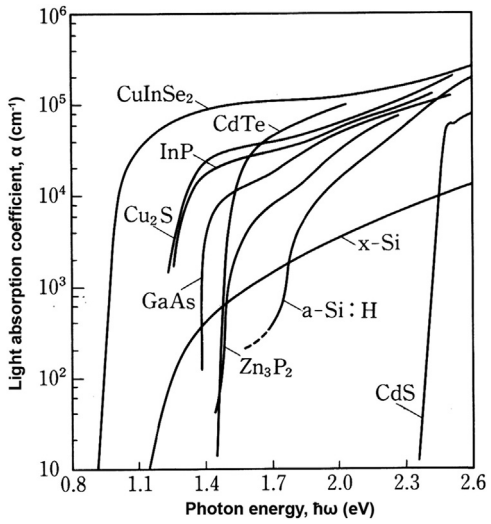

FIGURE 1.7

Light absorption coefficient spectra of semiconductors used in solar cells.

achievable conversion efficiency, $\eta_{\max}$, depends on these parameters. If we take the incident photon density of the solar radiation as a function of λ, $\Phi(\lambda)$ and the electronic charge as q, then the actually measured short circuit current I_{sc} will be as below.

$$I_{sc} = \int_0^\infty I_L(\lambda)d\lambda = qA\gamma(L_n + L_p)\int_0^\infty \varphi(\lambda)\alpha e^{-\alpha d}d\lambda \tag{1.7}$$

The short circuit current I_{sc} flows from the n-type region to the p-type region as seen in Fig. 1.5. The relationship between the terminal voltage V and flowing current I is the solar cell current-voltage characteristics as shown in the following Eq. (1.8), where the p region is regarded as positive.

$$I = I_0\left[\exp\left(\frac{qV}{nkT}\right) - 1\right] - I_{SC} \tag{1.8}$$

Here, I_0 is the reverse saturation current of the diode. Fig. 1.8 shows the output characteristics of the solar cell. Following the equation above, a voltage is produced per the light intensity when the terminals are in an open state. This voltage is termed as open circuit voltage, V_{oc}, as it becomes the following Eq. (1.9), where $I = 0$ (open circuit) in Eq. (1.8).

$$V_{oc} = \frac{nkT}{q}\ln\left(\frac{I_{sc}}{I_0} + 1\right) \tag{1.9}$$

As shown in Fig. 1.8, the maximum power point P_m is defined when the solar cell is connected to the optimum load R_L and the corresponding voltage and

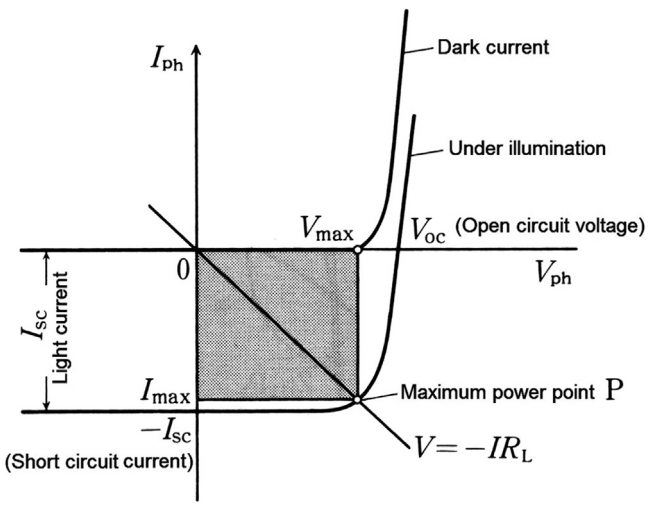

FIGURE 1.8

Current-voltage characteristics of the solar cell.

current are denoted by $V_{\max}$ (or V_{mp}) and $I_{\max}$ (or I_{mp}). The areas calculated by $V_{\max}$ and $I_{\max}$ are equivalent to the output power. Hence, following Eq. (1.8), P_{out} as the generalized output power of any solar cell is shown in Eq. (1.10).

$$\begin{aligned} P_{\text{out}} &= V \cdot I \\ &= V \cdot \left\{ Isc - I_0 \left[\exp\left(\frac{qV}{nkT}\right) - 1 \right] \right\} \end{aligned} \tag{1.10}$$

From Fig. 1.7, it is also clear that at the maximum power point $P_{\max}$ becomes,

$$\frac{dP_{\text{out}}}{dV} = 0 \tag{1.11}$$

Hence, from the above two equations, the maximum power-point voltage $V_{\max}$ satisfies the following relationship.

$$\exp\left(\frac{qV_{\max}}{nkT}\right)\left(1 + \frac{qV_{\max}}{nkT}\right) = \left(\frac{I_{sc}}{I_0}\right) + 1 \tag{1.12}$$

Meanwhile, the maximum power point current $I_{\max}$ can be expressed as the following.

$$I_{\max} = \frac{(I_{sc} + I_0) \cdot qV_{\max}/nkT}{1 + (qV_{\max}/nkT)} \tag{1.13}$$

In reality, the nominal energy conversion efficiency of any solar cell is measured under a solar spectra replicated light source that usually shows AM 1.5 and 100 mW/cm^2 for terrestrial application solar cells and AM 0 and 100 mW/cm^2 for space application solar cells. For instance, if all the parameters such as P ($V_{\max}$, $I_{\max}$) as well as V_{oc}, J_{sc} are found from a terrestrial application solar cells output characteristics measurement, the nominal conversion efficiency η_n for light exposed area S (cm^2) can be derived from the following equation.

$$\begin{aligned} \eta_n &= \frac{V_{max} \cdot I_{\max}}{P_{in} S} \times 100(\%) \\ &= \frac{V_{oc} \cdot J_{sc} \cdot FF}{100(\text{mW/cm}^2)} \times 100(\%) \\ &= V_{oc}(V) \cdot J_{sc}(\text{mA/cm}^2) \cdot FF(\%) \end{aligned} \tag{1.14}$$

where

$$\text{FF} = \frac{V_{\max} \cdot J_{\max}}{V_{oc} \cdot J_{sc}} \tag{1.15}$$

Here, FF is the curve fill factor (FF) or, simply, FF, which is the ratio between equivalent area of the maximum output power ($P_{\max}$) and the product of $V_{oc} \times J_{sc}$ as shown in Fig. 1.8, which also expresses the junction quality of the solar cell device.

Hence, the conversion efficiency of a solar cell is directly proportional to the I_{sc}, V_{oc}, and the FF during the performance evaluation where the input power (P_{in}) exposed to the solar cell is used as 1 kW/m^2 or 100 mW/cm^2.

1.6 Equivalent circuit of solar cells

The equivalent circuit of the solar cell has output characteristics as shown in Eq. (1.8), which is generally described with two components, the p-n junction diode's rectifying component and the constant current source component I_{sc} that depends on the intensity of incoming light. Apart from that, there are series resistances R_s that limit the terminal current and parallel resistances R_{sh} that facilitate the leakage current of the p-n junction part. All of these are shown in the equivalent circuit of the solar cell in Fig. 1.9. As shown in the figure, the solar cell terminal current and voltage are related by Eq. (1.16).

$$I = I_{sc} - I_0\left[\exp\left\{\frac{q(V + R_S I)}{nkT}\right\} - 1\right] - \frac{V + R_s I}{R_{sh}} \tag{1.16}$$

As shown from Fig. 1.9, for a particular solar cell at the time of lower light intensity and within the lower range of I_{ph}, the diode current I_d and the leakage current V_d/R_{sh} become almost equal. The solar cell equivalent circuit equation becomes Eq. (1.17), where it is more affected by R_{sh} than R_s.

$$I = I_{sc} - I_0\left[\exp\left(\frac{qV}{nkT}\right) - 1\right] - \frac{V}{R_{sh}} \tag{1.17}$$

On the contrary, in the case of higher light intensity, $I_d \gg V_d/R_{sh}$, the effect of R_s becomes more prominent than R_{sh} and the equation simplifies to (1.18).

$$I = I_{sc} - I_0\left[exp\left\{\frac{q(V + R_s I)}{nkT}\right\} - 1\right] \tag{1.18}$$

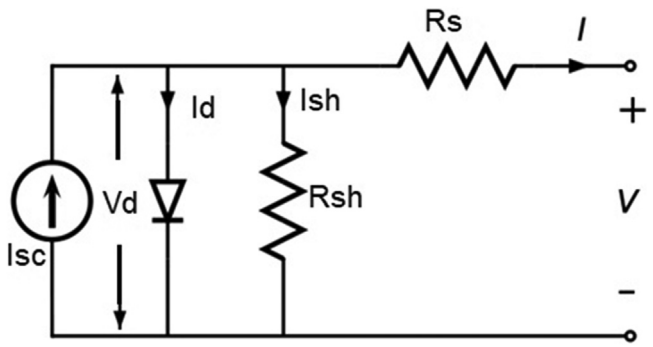

FIGURE 1.9

Equivalent circuit of the solar cell.

R_s does not have a significant effect on the open circuit voltage V_{oc}, whereas the short circuit current I_{sc} drastically decreases. Meanwhile, R_{sh} does not show any impact on I_{sc} but leads to a decrease in V_{oc}.

It is important to understand how the series resistance R_s affects the output current and can be shown with a simple example. In the case of silicon p-n junction solar cell, let us consider a short circuit current density J_{sc} of 30 mA/cm^2, I_o of 50 pA/cm^2, $n = 1$ at the incident power of 100 mW/cm^2. The calculation result of the R_s as the output parameter is based on Eq. (1.16), is shown in Fig. 1.10. In this case, the corresponding conversion efficiency is shown with respect to R_s values, whereby the shunt or parallel resistance is taken to be infinity to cause the leakage current to be 0. As seen, the solar cell output characteristics are largely affected by R_s. All of these can be explored in many of the available solar cell performance related simulation software. If we execute the same calculation taking R_{sh} as the variable parameter, the results are found as shown in Fig. 1.11. As seen from the figure, R_{sh} seems to affect the light-induced current comparatively less but V_{oc} has been largely affected. In basic silicon p-n junction solar cells, the V_{oc} is around 0.51 V. However, today's silicon solar cells are more complex in structure with back surface field as well as anti-reflection coatings with textured structures able to improve both V_{oc} and J_{sc} to reach over 25% conversion efficiency. Figs. 1.10 and 1.11 can be considered as the most important basic characteristics for R_s and R_{sh} as derived from the basic solar cell output characteristics calculation, which practically helps to understand the impacts of R_s and R_{sh} that may arise from various fabrication processes.

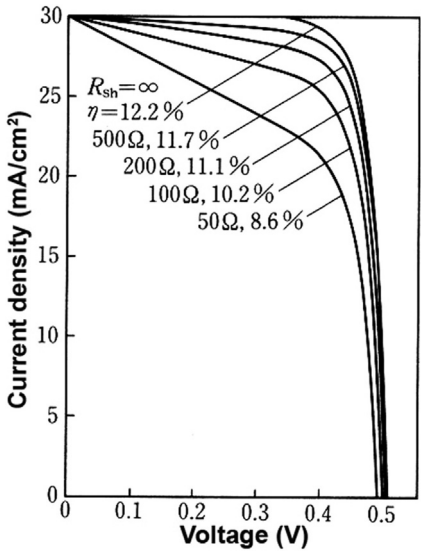

FIGURE 1.10

Output characteristics of a silicon solar cell at variable series resistances.

1.7 Collection efficiency

The carrier collection efficiency of a solar cell is an essential term that measures the spectra of generated carriers upon incident ideal sunlight and is then converted into the spectral response via the quantum effect (photon to electron energy transformation). It can be derived from the total number of carriers within the p-n junction upon solving the diffusion equation of the generated minority carrier. To provide effective carrier collection, wider bandgap semiconductors are used as window layers from where incident light enters either into heterojunction or heterointerface solar cells as shown in Fig. 1.12. Most

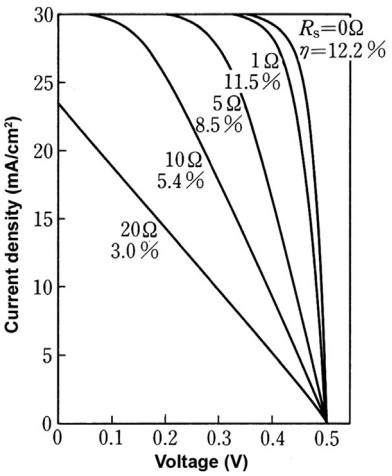

FIGURE 1.11

Output characteristics of a silicon solar cell at variable shunt resistances.

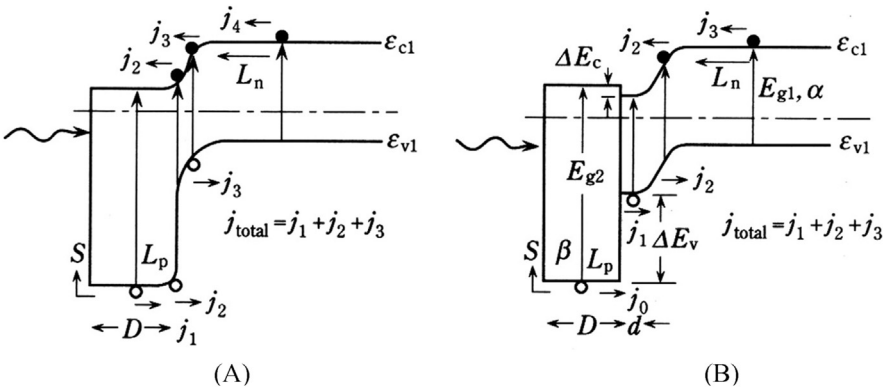

FIGURE 1.12

Band profile of solar cells with a wider window layer; (A) hetero junction solar cell and (B) hetero interface solar cell.

ideal heterojunction solar cells expect both the p and n regions to have the same doping concentration and that there is no inter-diffusion of carriers between them. However, in reality, the doping concentration is deliberately kept higher to reduce the resistance in the surface layer, which causes most of the hetero-junction solar cells to become hetero-interface solar cells. The basic difference in the carrier collection for both homo-junction and hetero-junction solar cells lies in the following fact. At a distance from the surface in both cases, the light intensity and collected carriers are found to be more improved for hetero-junction solar cells. However, structural design optimization is important for the materials to achieve higher conversion efficiency in hetero-junction solar cells, considering the complex interrelationship among the materials' bandgap and optical and electrical properties as well as matching the solar radiation energy spectra.

1.8 Theoretical limit of efficiency

In recent years, although the conversion efficiencies of solar PV devices have reached quite comparable values, a common question always arises as to why the efficiencies are not higher in comparison to other electrical power generating machines, for example, diesel generators. As we have learned some basics about conversion efficiency terminologies and equations in the above sections, we can now understand the sets of parameters involved in the efficiency measurement of the solar PV cells unlike conventional generators. Let's now look into the theoretical limit of solar cells, which involves two important facts: the materials used to absorb the sunlight and the incoming solar spectra. Ultimately, the overlapping between these two spectra, that is, absorption spectra of the main materials and the sunlight spectra, will decide the optimal limit of the solar cell device's performance. Fig. 1.13 shows some of the solar cell materials'

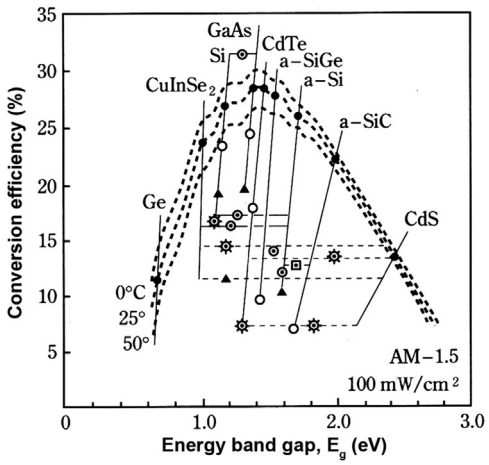

FIGURE 1.13

Theoretical efficiency limit of various kinds of solar cells at room temperature.

theoretical limits derived from the absorption spectra under AM-1.5, 100 mW/cm^2 incident light and practical data on the conversion efficiency observed in some materials, such as GaAs-based solar cells (theoretical limit is 28.5%). However, the calculation for the theoretical limit uses a simple structure for any light absorbing material, which may not be appropriate for all research-scale or commercially available solar cell. In the case of crystalline silicon solar cells, the theoretical limit for a single junction structure is 27%, whereas now many different configurations show greater than 26% efficiency. On the other hand, low cost amorphous silicon solar cells have theoretical limits around 25.5%; however, we have seen data in the 13%−15% range with some associated light-soaking degradation. Other thin film solar cells (TFSCs), such as CIGS (Cu-In-Ga-Se) or CdTe, also show 28% theoretical limits as found from different studies.

Nonetheless, the theoretical conversion efficiency limit is not greater than 30% for a single light absorbing material as discussed above. With the rigorous efforts of researchers around the world over the past few decades, the differences between the theoretical limits and practically achieved solar cells have moved closer with innovative structural engineering and light trapping technologies. The following discussion may help to understand the loss any solar cell incurs when exposed to sunlight spectra. At first, the conformity (overlapping) between the incident solar spectra and the spectral response of any solar cell that comes from the solar cell material's light absorption quality are very crucial. As mentioned earlier, the spectral response of any solar cell depends on the absorbing material's properties, such as bandgap and junction depth. In principle, the theoretical limit depends on the material property factor/constant that is bandgap, which exposes the inability of the light (photon) collection by the material as the resulting mismatch between the solar spectrum and spectral response of the material. More clearly, these are losses that correspond to light moving through the solar cell without being absorbed and the light that is reflected or scattered from the surface of the solar cell. Apart from these collection losses, the other overlapping part can be fully utilized for photon to electron excitation or solar cell effects in spite of several loss mechanisms. Among the losses that limit the collection efficiency of solar cells, they can be classified in the following categories:

1. Light reflection loss from the surface even though collectible by spectral response
2. Surface recombination loss of the carriers generated by the collected light (photon)
3. Bulk recombination loss of the carriers in the semiconductor bulk
4. Series resistance loss due to the Joule heat produced by the internal carrier flow (current)
5. Voltage factor loss due to the polarized electric field by the light generated carriers limited by the p-n junction's diffusion voltage V_d, where photons equivalent to bandgap energy encounter loss of hν-qV_{oc} ($qV_{oc} < qV_d < E_g$)

The key factor to improving the efficiency of solar cells depends on the above mitigation of loss mechanisms using various innovative techniques.

1.9 Classification of solar cells

Solar cells can be classified in many ways, such as the generation or based on the main light absorption materials in the physical structure. Although solar cells were first designed for very specialized uses such as in spacecrafts and satellites, they can now be found in everyday use, such as wristwatches to central power stations. The development of the solar cell originates from the work of French physicist Alexander Edmond Becquerel in 1839. He discovered the PV effect while experimenting with a solid electrode in electrolyte solution. He observed that when light fell upon the electrode, voltage developed. The discovery of photoconductivity in selenium led to the fabrication of the first selenium solar cell by W.G. Adams in 1877. In 1883, the first true solar cell that was only around 1% efficient was built by Charles Fritts who coated the semiconductor selenium with a very thin and transparent layer of gold to form the junction. Another metal semiconductor junction solar cell, which was made of copper and semiconductor copper oxide was demonstrated in 1927. By 1930, both the selenium cell and copper oxide cell were being employed in light-sensitive devices, such as photometers for photography. These early solar cells had energy-conversion efficiencies of less than 1%. This standoff was finally overcome with the development of the Si solar cell patented by Russell Ohl in 1941.

The modern age of solar power technology arrived in 1954 when Bell Laboratories, experimenting with semiconductors, accidentally found that silicon doped with certain impurities was very sensitive to light. In 1954, three American researchers, namely G.L. Pearson, Daryl Chapin, and Calvin Fuller, demonstrated a 6% efficient silicon solar cell when used in direct sunlight, which increased to 14% by 1958 and 28% by 1988. In the same year, the first thin film Cu_2S/CdS heterojunction solar cell with 6% efficiency was reported by Reynolds. In 1956, Jenny reported a GaAs solar cell with 4% conversion efficiency. In 1963, D.A. Cusano fabricated the first thin film CdTe solar cell based on CdTe/Cu_2Te heterojunction with 6% efficiency. Bonnet and Rabenhorst reported a thin film CdTe/CdS solar cell in 1972 with 6% efficiency. In 1974, S. Wagner et al. reported a thin film $CuInSe_2$/CdS heterojunction solar cell with 12% conversion efficiency. However, the 1980s and 1990s have been a period in which public and governmental support for PVs has been underemphasized, but significant activity in the research community has continued. Generally speaking, solar PV technology can be classified into three generations, as explained in subsequent sections and shown in Fig. 1.14.

1.9.1 First generation solar cells

First generation solar cells are made of semiconducting p-n junctions consisting of silicon. Silicon cells have a high efficiency averaging 20%, but very pure

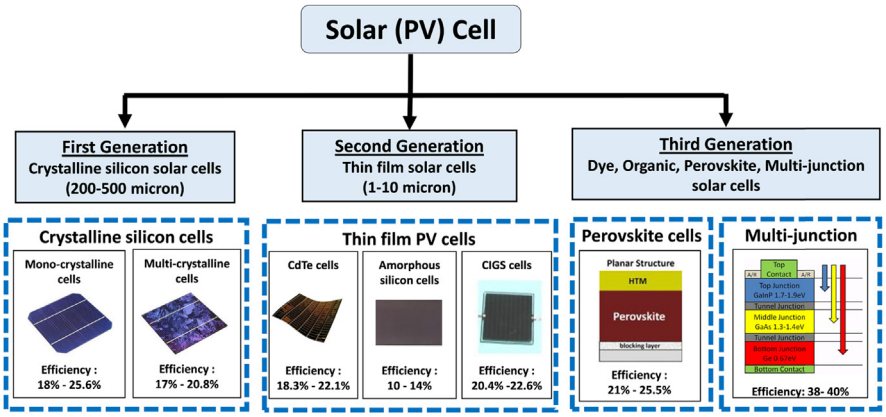

FIGURE 1.14

Solar cell classification.

silicon is needed and the price is high when compared to the power output. These solar cells are manufactured from pure silicon and their theoretical efficiency can reach a maximum of 33%. First generation solar cells account for over 90% of commercial production and include both mono and multicrystalline silicon. However, in recent years, a "directionally solidified (DS) wafer" (also called a "cast mono" wafer) has been developed that is different than the usual Czochralski growth process and has slowly replaced mainstream mono-crystalline silicon. The manufacturing processes associated with the production of first generation solar cells are still inherently expensive; hence, these cells may take 5–6 years to pay back their initial investment.

1.9.2 Second generation solar cells

Second generation solar cells are based on reducing the cost of first generation cells by employing thin film technologies. Thus, TFSCs have been regarded as a potential low cost, high efficiency solar cell which can replace Si solar cells in the PV market. The obvious advantages of TFSC over Si solar cells are low temperature processing techniques, low material usage, a variety of deposition processes and its compatibility with low cost substrates. Combining all of these advantages, low cost PV cells are achievable and suit the criteria for large scale applications, such as terrestrial deployment. Types of solar cells that fall under the TFSC category are cadmium telluride (CdTe), copper-indium-gallium-diselenide (CIGSe), copper-zinc-tin-sulfide (CZTS) and amorphous silicon (a-Si) solar cells. CdTe, CIGS, and amorphous silicon TFSCs entered the commercialization stage over 20 years ago.

1.9.3 Third generation solar cells

Third generation solar cells have been developed to enhance the average optoelectronic conversion performance of second generation technology while maintaining low production costs. The goals are to promote thin-film solar cells that use novel approaches to obtain efficiencies in the range of 30%−60%. Dye-sensitized solar cells once flourished to some extent for low cost approaches with great expectations. In recent years, Gratzel and his co-workers achieved 10.9% conversion efficiency using organometal lead halide perovskites as an alternative to dye-sensitized solar cells. The structure of the device is a simple heterojunction thin film. Organo metallic lead halide perovskite ($CH_3NH_3PbI_3$) is currently a leading thin film material for its numerous beneficial properties to realize low cost and high efficiency solar cells. $CH_3NH_3PbI_3$ (bandgap: 1.5 eV) has a high absorption coefficient of over $10^5\,cm^{-1}$, which means that all the potential photons of sunlight with energy greater than the bandgap can be absorbed within the 400-nanometer thick $CH_3NH_3PbI_3$ absorber layer. On the other hand, there are a few more approaches that can improve the efficiency such as spectrum splitting (multi junction solar cells), incident spectrum modification (by using concentrators), multiple electron-hole pair generation by a single photon and some others. Technologies associated with third generation solar cells include multi-junction PV cells, tandem cells, and nano-structured cells to pick up better incident light and convert excess thermal energy to improve voltages or carrier collection.

Nonetheless, there are various PV cells that show different light absorbing materials, structures, and associated fabrication methods. Table 1.1 shows the highest confirmed research scale cell results. These highest confirmed efficiencies have been published under the title of "Progress in Photovoltaics" since 1993 that provide an authoritative summary of the current state-of-the-art. The latest version, 56, was published in 2020.

1.10 Efficiency measurement

Solar cell efficiency is always misinterpreted or speculated for yield. Efficiency is measured from the solar cell's current voltage characteristics at defined standard illumination conditions, but the yield is the outdoor performance of any solar cell or panel for its promised output at standard conditions. Again, solar cell current-voltage characteristics are influenced not only by incident light intensity but also the spectra used for the measurement to replicate sunlight. Therefore, careful consideration is needed to minimize the error margin in the performance measurement. Measuring the characteristics under perfect standard conditions or at a given condition needs special skill. Solar cell efficiency measurement depends on the precise spectral content of the sunlight that fluctuates with the AM, moisture content, turbidity, etc. It is really not appropriate to use natural sunlight as the

Table 1.1 Confirmed non-concentrating terrestrial PV cell efficiencies measured under the global AM1.5 spectrum (1000 W/m^2) at a cell temperature of 25°C (IEC 60904−3: 2008 or ASTM G-173−03 global).

Classification	Eff. (%)	V_{oc} (V)	J_{sc} (mA/cm^2)	FF (%)	Description/reference
Silicon					
Si (Crystalline)	26.7 ± 0.5	0.738	42.65	84.9	Kaneka, n-type rear IBC
Si (DS: Directionally Solidified)	24.4 ± 0.3	0.7132	41.47	82.5	Jinko Solar, n-type
III-V Cells					
GaAs (thin-film)	29.1 ± 0.6	1.1272	29.78	86.7	Alta Devices
GaAs (multicrystalline)	18.4 ± 0.5	0.994	23.2	79.7	RTI, Ge substrate
InP (crystalline cell)	24.2 ± 0.5	0.939	31.15	82.6	NREL
III-V Cells					
GaAs (thin-film)	29.1 ± 0.6	1.1272	29.78	86.7	Alta Devices
GaAs (multicrystalline)	18.4 ± 0.5	0.994	23.2	79.7	RTI, Ge substrate
InP (crystalline cell)	24.2 ± 0.5	0.939	31.15	82.6	NREL
Thin-Film Chalcogenide					
CIGS (Cd Free)	23.35 ± 0.5	0.734	39.58	80.4	Solar Frontier
CdTe (cell)	21.0 ± 0.4	0.8759	30.25	79.4	First Solar, on glass
CZTSSe (cell)	11.3 ± 0.3	0.5333	33.57	63.0	DGIST, Korea
CZTS (cell)	10.0 ± 0.2	0.7083	21.77	65.1	UNSW
Amorphous /microcrystalline Si					
Si (amorphous)	10.2 ± 0.3	0.896	16.36	69.8	AIST
Si (microcrystalline)	11.9 ± 0.3	0.550	29.72	75.0	AIST
Perovskite					
Perovskite cell	21.6 ± 0.6	1.193	21.64	83.6	ANU
Dye-sensitized					
Dye (cell)	11.9 ± 0.4n	0.744	22.47	71.2	Sharp
Organic					
Organic (cell)	15.2 ± 0.2	0.8467	24.24	74.3	Fraunhofer ISE
Multijunction Devices					
Five-junction cell (bonded) (2.17/1.68/1.40/1.06/0.73 eV)	38.8 ± 1.2	4.767	9.564	85.2	Spectrolab, two terminal

Edited from Green, M. A., Dunlop, E., Hohl-Ebinger, J., Yoshita, M., Kopidakis, N., & Hao, X. (2020). Solar cell efficiency tables (version 57). Progress in Photovoltaics: Research and Applications*, 2020; 1−13 (Green et al., 2020).*

input light as natural light largely varies depending on the location, atmospheric conditions, seasonal variation, incident angle, luminance, and spectral irradiance. Here, the most recommended efficiency measurement method will be introduced, which uses replicated sunlight. In this case, the standard sunlight distribution to which measurements are referenced is the AM1.5 distribution of Fig. 1.1. Solar simulators are employed as recommended light sources as close as AM1.5 spectral distribution using a filtered xenon lamp, ELH lamp, and even LEDs nowadays. Whatever the light source used, the illumination source must give a collimated beam of uniform intensity at the test plane with stability at the time of measurement within the specified limit.

A typical experimental setup for measuring current-voltage characteristics is shown in Fig. 1.15. It is more desired to have a four-point probe measurement scheme to keep current and voltage probes separate to the device under testing to eliminate the effects from series resistance as well as contact resistances. The PV cell should be kept at 25°C throughout the measurement time with complete shutdown of other light interferences except the solar simulator light. The lamp intensity can be calibrated using a reference cell measured under standard conditions elsewhere. The current-voltage characteristics can then be measured by using variable load resistance to the device under test, that is solar PV cell.

There is another kind of important measurement of solar cells, which is the spectral response of the cell. It is the direct comparison of the output of a cell with the calibrated spectral response. A steady-state source of monochromatic light from a monochromator can be used as the simplest method. It gives the carrier generation or simply current response of the solar cell for each light wavelength with the closest intensity of sunlight replication. The ultimate spectral response of the solar cell would match with the short circuit current density, if properly measured in both methods.

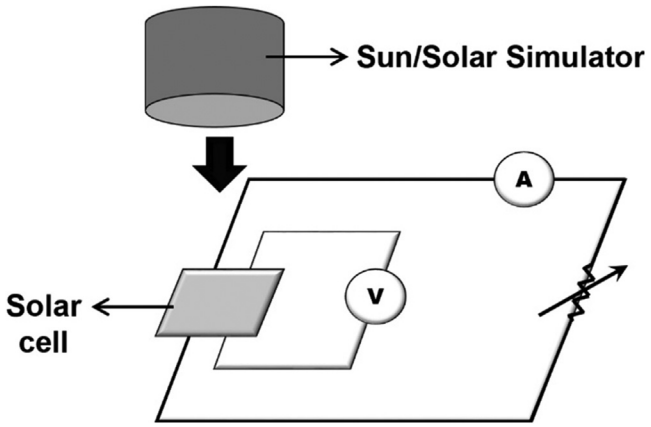

FIGURE 1.15

A typical experimental setup for measuring current-voltage characteristics.

1.11 Summary

Sunlight is continuously pouring down, free of cost, which can more than sustain our existence on earth. Apart from making livable conditions on earth, solar energy can be harnessed as the most efficient form, that is, electricity to cater all our needs using a solar cell. Sunshine that reaches the earth varies drastically and unpredictably in terms of availability, intensity, and spectral composition; however, solar cells of various available materials can convert substantial amounts of sunlight through a phenomenon called the PV effect. Around 98.98% of energy that can be collected on earth comes from solar energy and the remaining 0.02% comes from geothermal energy. As discussed in this chapter, the solar energy sent to earth is 10,000 times more than mankind's average usage. Solar PV devices were realized based on the discovery of the PV effect in the 19th century, but momentum has slowed over the past 70 years. Compared with other energy sources, solar PV energy systems do not require moving parts and silently produces clean energy free of GHG emissions with minimal maintenance. Expansion or scale-merit is better than any others due to the addition of solar panels for any expansion. Based on known physics and the adoption of novel technology for the materials and structures, solar cells have evolved dramatically in recent times having light to electricity conversion efficiencies increase from 6% (single cell) to nearly 50% (tandem). Novel PV materials are being researched extensively, and larger solar farms are being established around the world. A majority of countries have optimistically incorporated around 50% of their annual energy sources to be solar PV energy for their energy roadmap by 2050. It is hoped that the fundamental discussion in this chapter assists the readers to a level that they can easily follow the subsequent chapters on other topics related to PV energy technologies.

Acknowledgments

The author wishes to thank the Ministry of Higher Education of Malaysia (MOHE) for providing the research grant with the code of LRGS/1/2019/UKM-UNITEN/6/2 to support our research activities on solar photovoltaic energy. Appreciation is also give to the Universiti Tenaga Nasional (UNITEN) for providing substantial support on solar energy related R&D over the years.

References

Green, M. A., Dunlop, E., Hohl-Ebinger, J., Yoshita, M., Kopidakis, N., & Hao, X. (2020). Solar cell efficiency tables (version 57). *Progress in Photovoltaics: Research and Applications*, *2020*, 1–13. doi:10.1002/pip.3371.

Further reading

Green, M. A. (1998). *Solar cells: Operating principles, technology and systems applications*.

Hamakawa, Y., & Kuwano, Y. (1994). *Solar enegy engineering: Solar cells*. Baifukan Publications.

Manabe, S., & Stouffer, R. J. (1980). *Journal of Geophysical Research*, *85*(1980), 5529.

Nelson, J. (2008). *The physics of solar cells*. Imprerial College Press.

Thekackara, M. P. (1970). The solar constant and the solar spectrum measured from a research aircraft. NASA Technical Report No. R-351.